Geophysical Journal International

Geophys. J. Int. (2010) **182,** 1–10 doi: 10.1111/j.1365-246X.2010.04595.x

The bright spot in the West Carpathian upper mantle: a trace of the Tertiary plate collision—and a *caveat* for a seismologist

Piotr Środa

Institute of Geophysics, Polish Academy of Sciences, Ks. Janusza 64, 01-452 *Warsaw, Poland. E-mail: psroda@igf.edu.pl*

Accepted 2010 March 9. Received 2010 January 29; in original form 2009 October 28

SUMMARY

The 2-D full waveform modelling of the mantle arrivals from the CELEBRATION 2000 profiles crossing the Carpathian orogen suggests two possible tectonic models for the collision of ALCAPA (Alpine-Carpathian-Pannonian) and the European Plate in the West Carpathians in southern Poland and Slovakia. Due to an oblique (NE-SW) convergence of plates, the character of the collision may change along the zone of contact of the plates: in the western part of the area an earlier collision might have caused substantial crustal shortening and formation of a crocodile-type structure, with the delaminated lower crust of ∼100 km length acting as a north-dipping reflecting discontinuity in the uppermost mantle. In the eastern part, a less advanced collision only involved the verticalization of the subducted slab remnant after a slab break-off. The lower crustal remnant of ∼10 km size in the uppermost mantle acts as a pseudo-diffractor generating observable mantle arrivals. Due to the similarity of synthetic data generated by both models, the question of the non-uniqueness of seismic data interpretation, that may lead to disparate tectonic inferences, is also discussed.

Key words: Controlled source seismology; Continental tectonics: compressional; Crustal structure; Europe.

1 INTRODUCTION

The convergence of continental plates, manifested as subduction and collisional processes, leaves a signature in the structure of the lithosphere. Seismic studies of the orogens focus on recovering this imprint to allow for tracing back the tectonic evolution of the orogen and to help our understanding of the processes of formation of the convergent structures in general. The Carpathians provide an excellent opportunity to investigate the evolution of a compressional mountain chain. The structure of the Carpathian lithosphere was recently studied within the scope of the CELEBRATION 2000 experiment (Guterch *et al.* 2001). Four seismic refraction and wide-angle reflection profiles are located across the Carpathian orogen in southern Poland and Slovakia—CEL01, CEL04, CEL05 and CEL11 (Grad *et al.* 2006; Środa *et al.* 2006; Janik *et al.* 2009). This provided constraints for the seismic velocities of the Carpathian crust and upper mantle and allowed for a study of the differences between the structure of the orogen and the neighbouring areas—the East European Craton (EEC), the Małopolska Unit (MU) and the Brunovistulian Unit (BSU) in the North, and the Pannonian Basin System (PBS) in the South. The seismic data were interpreted by 2-D trial and error ray tracing modelling technique. Apart from establishing models of V_p velocity down to *ca.* 50 km depth, these studies revealed high apparent velocity arrivals, which were interpreted as reflections from a north-dipping discontinuity in the uppermost mantle. However, further research suggested another possible origin of these mantle phases, therefore amplitude modelling in addition to kinematic interpretation was applied to study their nature, including off-line recordings to enlarge the data set. The current work focuses on 2-D finite-difference amplitude modelling of these mantle arrivals, presents models of the present structure of the Carpathian arc as a result of plate convergence and attempts to trace back the evolution of a subduction-collisional orogen. The results justify the consideration of two alternative solutions for the origin of the modelled phases, suggesting two likely scenarios (or two stages) for subduction cessation and collision in the Tertiary. This also has an important bearing on the philosophy of seismic interpretation in cases when a divergent outcome, leading to disparate tectonic inferences, cannot be excluded.

2 GEOLOGY

The Western Carpathians are the northernmost part of the Alpine orogenic system in Europe. Their structure resulted from the Late Jurassic to Tertiary oblique southward subduction of oceanic domains, taking place between the old European plate and mobile fragments of continental lithosphere of the Apulia/Adria in the south, and from a further collision of these plates. (Plašienka *et al.* 1997a). According to Tomek & Hall (1993), the Western Carpathian subduction was ended by a slab detachment in the Late Tertiary.

The northern foreland of the Carpathians—the European Platform—encompasses the Proterozoic EEC, as well as BSU and

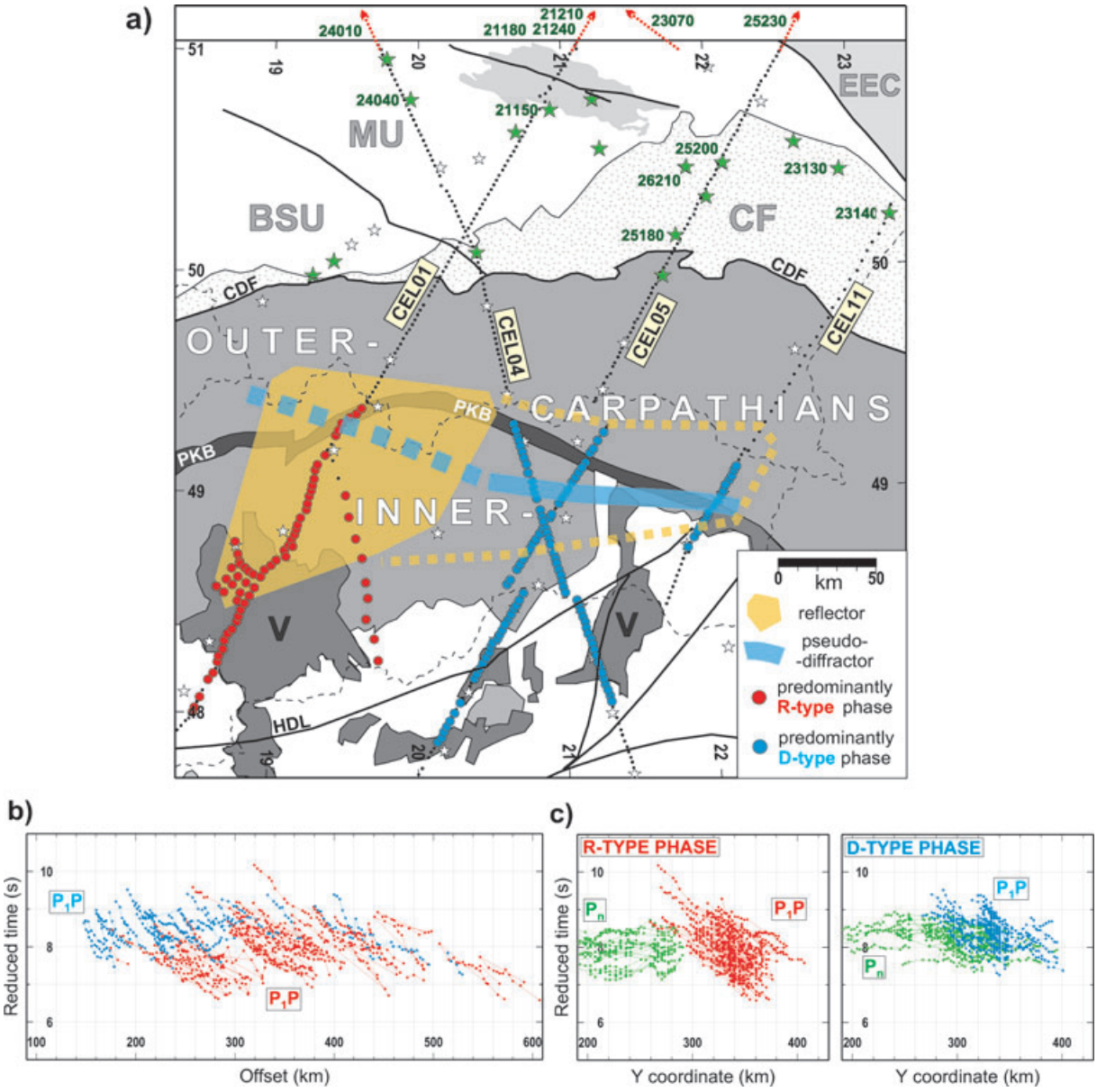

Figure 1. (a) Tectonic map of the study area and localization of the seismic profiles. Green stars, shot points used for the study; white stars, other shot points; red and blue points, receivers recording the P_1P phase; EEC, East European Craton; MU, Małopolska Unit; BSU, Bruno-Silesian Unit; CF, Carpathian Foredeep; V, Neogene volcanites; PKB, Pieniny Klippen Belt; CDF, Carpathian Deformation Front; HDL, Hurbanovo-Diósjenö Line. (b) Traveltimes of the P_1P phase. (c) P_1P traveltimes subdivided into R- and D-type. Reduction velocity is 8 km s^{-1}.

MU, consolidated in Palaeozoic times (Fig. 1a). The collisional fold-belt of the Western Carpathians consists structurally of the Outer West Carpathians (OWC) in the North and Inner West Carpathians (IWC) in the South, separated by the Pieniny Klippen Belt (PKB). The PKB is considered as a surface expression of the Late Cretaceous to Early Tertiary closure of the Vahicum (Penninic related) oceanic domain (Plašienka *et al.* 1997a, Mahel' 1981). It is a 1- to 20-km-wide strip composed largely of Jurassic/Cretaceous limestone formations, considered to be detached from an unknown basement, with Palaeogene overstep sequences. Another presumed oceanic suture in the Catpathians is the Late Jurassic Meliata suture in the IWC, located along the Raba-Hurbanovo-Diósjenő Line.

The Outer Carpathians, bordered in the north by the Neogene molasse sediments of the Carpathian Foredeep, are composed of Carpathian flysch sedimentary nappes of the Late Jurassic to Tertiary age, thrusted northwards over the Palaeozoic to Early Mesozoic margin of the European Plate basement and forming an orogenic accretionary wedge. The flysch sediments measure over 10 km in thickness at the PKB and thin out northwards to the Carpathian Thrust front about 80 km from the PKB (Środa *et al.* 2006).

The Inner Western Carpathians (Fig. 1a) consist of three main thick-skinned crustal units: Tatricum, Veporicum and Gemericum, consisting of the pre-Alpine (partially Variscan) crystalline basement and Palaeozoic sequences, covered by Late Palaeozoic/Triassic nappe systems. The IWC were subject to extensive crustal shortening during the Cretaceous (Plašienka *et al.* 1997b). The southern part of the IWC is partially covered by Tertiary sediments of the Pannonian Basin System and Neogene volcanics. The volcanics are represented by Early Miocene areal rhyolites and dacites,

related to early back-arc spreading, Middle Miocene island-arc type andesites connected with the retreating subduction of the oceanic lithosphere beneath IWC, and alkali basalts of Late Miocene age, originated due to post-subduction extension and asthenosphere updoming (Kováč *et al.* 1997; Lexa & Konečný 1998). The geochemistry and spatial location of the volcanic areas in the IWC, timing of their activity and the geometry of the overthrust OWC nappes, are strong proof for the concept of a southward subduction of the oceanic crust of the European Platform beneath the Apulia-Adria. They suggest also a verticalization of the subducting slab with time, and a possible detachment of the sinking slab prior to a subsequent collision. The location of actively subducting segment migrated along the subduction zone from the West to the East (Lexa & Konečný 1998).

The thickness of the crust changes across the Carpathian arc from 25 to 30 km in the PBS in the South, through 35–43 km beneath the OWC/IWC boundary (PKB) (Środa *et al.* 2006; Grad *et al.* 2006), to 30–45 km north of OWC. The Moho depression seems to be confined to the central part of the Western Carpathians, as it is observed only beneath the CEL01 and CEL04 profiles. The thickness of the Carpathian lithosphere, inferred from seismic (Babuška & Plomerová 2006) and gravity studies (Zeyen *et al.* 2002) varies substantially—from 50 to 60 km in the PBS, through *ca.* 100 km in Carpathians (120 km beneath the lithospheric root in the central part), to 180–200 km in the north. For a summary of other previous geophysical investigations, see Środa *et al.* (2006).

3 DATA

The analysis of the wide-angle data from CELEBRATION 2000 revealed strong mantle arrivals of unusually high apparent velocity (*ca.* 9 km s^{-1} or more), observed for ray paths crossing the Carpathian orogen from the north. The amplitude of this phase (called here P_1P) is usually higher, or at least equal, to the P_n amplitude (Fig. 2). At large offsets (>300 km) the phase is clearly visible even if the P_n phase is not observed at all. This suggests a 'bright spot' in the uppermost mantle of the Carpathians, turning up the waves propagating in the mantle back to the surface with considerable amplitude. The P_1P phase is observed along profiles CEL01, CEL04, CEL05 and CEL11 (Środa *et al.* 2006; Grad *et al.* 2006) in the in-line and off-line recordings of 43 shots from various profiles. The shots generating these arrivals are mostly located North of Carpathians, in the area of the Małopolska Unit and EEC (except a few shots located in the eastern IWC). Independently of the shot location, the high velocity P_1P arrivals are consistently observed in approximately the same area—beneath the IWC in the distance range of 0–150 km from the PKB, and for a wide range of offsets from the shot points (200–600 km) (Figs 1b and c). Confinement to a specific geographical location and high apparent velocity ($\geq$9 km s^{-1}) suggest that this phase originates from a localized feature, situated in the uppermost mantle approximately beneath the Outer and Inner Carpathians, acting as a secondary source of high amplitude waves. Structures with a larger extent (e.g. a long subhorizontal discontinuity) would produce reflections in approximately the same offset range, but at different coordinates along the profiles, unlike those observed here.

The 2-D modelling along CEL01 and CEL04 profiles (Środa *et al.* 2006) interpreted this phase as a reflection from a north-dipping discontinuity with a high impedance contrast, extending over a *ca.* 150 × 150 km large area and dipping from a depth of 45 km in the south to 70 km in the north, approximately perpendicularly to the strike of the Carpathian arc. However, analysis of all observed P_1P recordings (*ca.* 130 record sections, approx. 1700 traveltimes) shows some systematic differences in P_1P properties (apparent velocity, amplitude and shape of the traveltime curve) according to location. Based on this, two classes of the P_1P arrivals were isolated, as end-members for the rest of arrivals with intermediate characteristics (Figs 1b and c).

The first class, representative for the data recorded in the western part of the area (CEL01 profile), as well as for CEL04 and CEL05 recordings of the shots in the West, forms a long (70–100 km) series of arrivals, possible to fit by a straight line with an apparent velocity of *ca.* 9 km s^{-1} (Fig. 2). The P_n phase is usually weak or not observed. When visible, P_n often vanishes at offsets where P_1P starts to be visible. This can be due either to its low amplitude relative to strong P_1P, which effectively makes P_n invisible on trace-normalized record sections, or may be the effect of a local increase of attenuation at the Moho, preventing further propagation of the P_n phase. Such arrivals, observed later or at larger offsets than the P_n phase, are usually interpreted as reflections from mantle discontinuities. Therefore, this class of arrivals is likely to represent reflections from a north-dipping mantle discontinuity (R-type phase).

Other class of arrivals, observed for northern and eastern shots recorded along the profiles CEL04, CEL05 and CEL11, shows short (20–50 km) series of pulses with high amplitude and apparent velocity over 9 km s^{-1}, forming lines with significant curvature on the x-t plot (Fig. 2). With increasing offset, this phase merges quickly with preceding weaker P_n phase. Such traveltime characteristics are similar to arrivals generated by a point diffractor located immediately below the refracting discontinuity (or for reflections from very steeply inclined discontinuity) and will be called here 'D-type' phases. Some seismic sections show phases with properties intermediate between the R-class and D-class.

4 MODELLING METHOD

To determine the nature of the 'bright spot' and the possible mechanism of generating these two classes of phases, a modelling of relative amplitudes of the P_1P and P_n phase was applied, together with traveltime modelling which helped to limit the range of possible models to a subset that fits observed traveltimes. For amplitude modelling of the wavefield, a finite-difference full waveform calculation was used. The MPM code (Hansen & Jacobsen 2002) allows for the computation of a limited portion of the wavefield in a moving zone containing the needed segment of the wave front. This feature is particularly useful in case of wide-angle data and allows for considerable savings in memory requirement and computation time. The code uses fourth-order space and second-order time FD solver of the elastic wave equation. The velocity/density model was parameterized on a 2-D grid with 200 m spacing. The dominant frequency of the calculated wavefield was 4 Hz. A synthetic noise was added to the calculated seismograms to simulate the real data signal-to-noise ratio. The background velocity models for full waveform calculations were prepared using traveltime trial-and-error forward modelling with ray tracing code SEIS83 (Červený & Pšenčík 1983) based on published CEL01, CEL04 and CEL05 models (Środa *et al.* 2006; Grad *et al.* 2006) to obtain a V_p velocity field which realistically simulates crustal and upper mantle structure by fitting the traveltime data. The original models were subject to the smoothing of the crustal velocity field to avoid strong reverberations from crustal discontinuities, in particular from the sedimentary layers. As the original models were prepared based on in-line shots

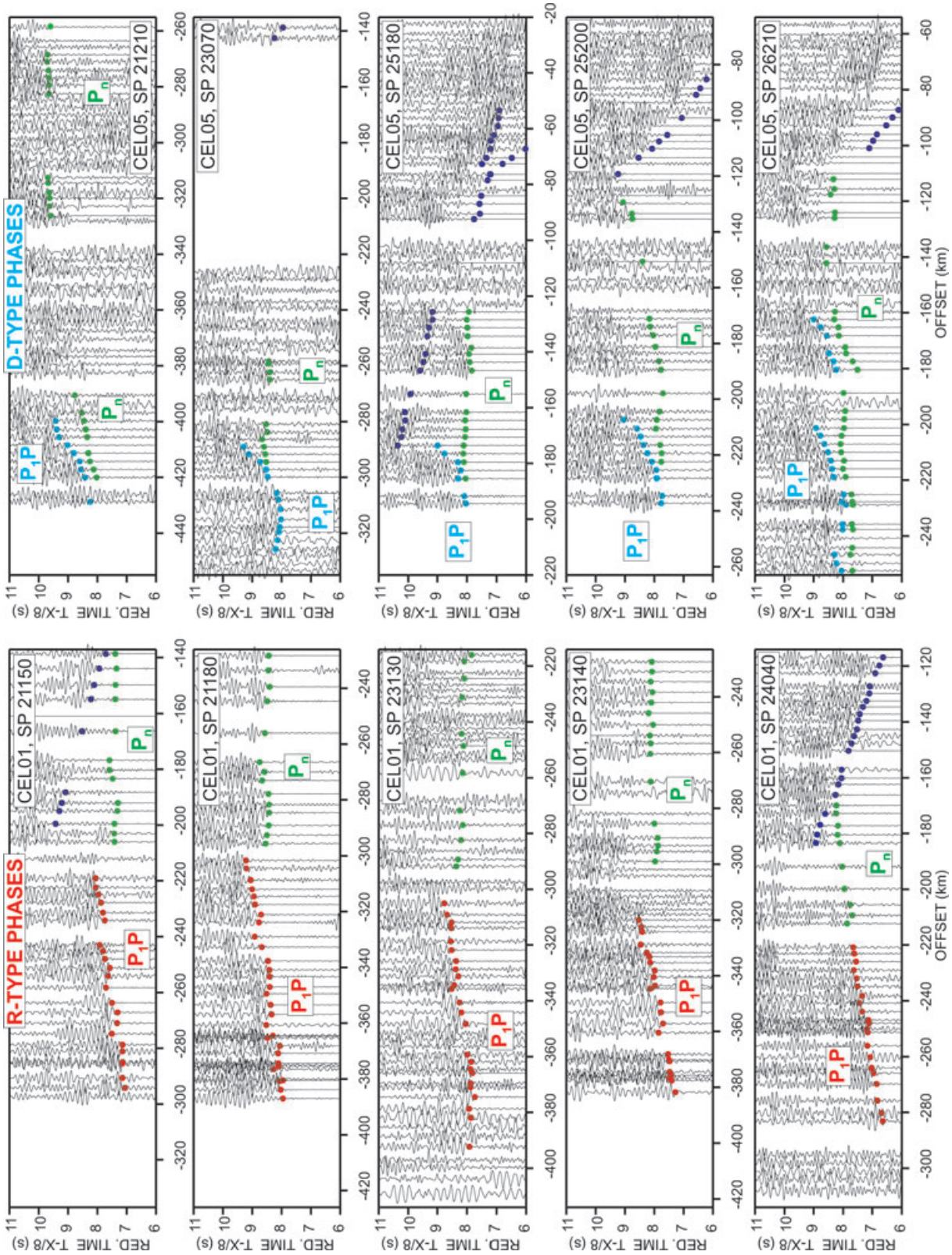

Figure 2. Examples of trace-normalized seismic sections with R- and D-type P_1P arrivals. Reduction velocity is 8 km s^{-1}.

and 2-D geometry, modelling of the off-line shots required adjusting the model structure near the shots to account for the fact that crustal structure at shots located far from profile could be significantly different than in the original 2-D models. Mantle V_p velocity was set to a constant value of 8.05 km s^{-1} (for some models—with negative V_p gradient—0.006 s^{-1}) down to 60 km depth, with a 0.003 s^{-1} vertical V_p gradient below this depth. Background models were modified by introducing several variants of structures in the uppermost mantle to generate a synthetic P_1P phase, which fits best the amplitudes of the observed P_1P.

5 MODELLING AND RESULTS

The full waveform modelling involved two main classes of models: a northward inclined reflecting discontinuity of 50–150 km length connected with the crust at 70–130 km distance to the south of the PKB (R-type models) (Figs 3 and 4), and a small size (of the order of 10 km) velocity anomaly at the Moho located beneath or close to the PKB (0–30 km distance), simulating a feature diffracting waves from the uppermost mantle (D-type models) (Figs 3 and 5).

In the R-class of models, several thicknesses of the reflector (0.5, 1, 2, 5 and 10 km) were tested, as well as several V_p contrasts relative to neighbouring mantle: +0.5, −0.5 and −1.0 km s^{-1}. In the D-class, the pseudo-diffractor was designed as a rectangular area with V_p lower (6.8 km s^{-1}—lower crustal velocity) or higher (8.5 km s^{-1}) than the mantle, connected with the base of the crust (Fig. 3). The size of this low velocity anomaly was 5–20 km horizontally and 5–15 km vertically. Other shapes of the anomaly—circular, irregular, trapezoidal, right- and left-dipping, detached from the crust, were also tested. The tests showed that the shape of the anomaly does not significantly influence the main characteristics of the wavefield.

Therefore, in this work, modelling results are presented for a rectangular anomaly shape, however, it should be noted that this is just a schematic representation of a low velocity uppermost mantle anomaly that can as well be of an irregular shape. The modelling allows us just to estimate the size and depth of the anomaly. Similarly, the R-class models, with a dipping discontinuity, are a schematic representation of another class of the mantle anomalies, characterized by its considerable horizontal extent (of the order of 100 km compared to <20 km for D-class), and by its northward dip. For reflector type models, an acceptable fit of amplitudes was achieved for a discontinuity thickness of 1–5 km, and both a positive (+0.5 km s^{-1}) and negative (−1.0 km s^{-1}) velocity contrast produced similar amplitudes. In this work, results are presented for a 1-km-thick discontinuity with V_p contrast of −1.0 km s^{-1} (Fig. 3). The pseudo-diffractor models required a negative velocity contrast at the anomaly (V_p of 6.8 km s^{-1})—the positive contrast (V_p of 8.5 km s^{-1}) generated a very weak P_1P phase. The best fit was obtained for an anomaly size of 10 × 5 km (CEL04 and CEL05 profile) and 10 × 8 to 15 × 8 km for the CEL01 profile. On few seismic sections, we can observe more than one high velocity phase—for example, for SP 26210, CEL01 (Fig. 5), three short P_1P-type phases were correlated. They are best modelled with a variant of a D-type model containing three pseudo-diffractors at ∼50 km from each other.

Interestingly, the results suggest that when the amplitude fit is concerned, both R-class and D-class data can fit reasonably well to either reflector or pseudo-diffractor models (Figs 3–5). However, when the shape and curvature of the traveltime trend of the P_1P is considered, R-class data (the long, linear phases) seem to be better represented by the reflector model, whereas D-class arrivals (short, high curvature phases) favour the pseudo-diffractor model. Nevertheless, in each case alternative solution cannot be totally excluded, at least for some subset of the data. This ambiguity is notable because even if non-uniqueness is always inherent to seismic modelling, in this case it does not mean just the uncertainty of model parameters, but it leads to two qualitatively different solutions.

The modelling shows that the mantle structure in the western part of the area is well described by a model of a dipping reflecting discontinuity, while for the eastern part the model of a pseudo-diffractor at the Moho boundary is more applicable. It is worth to compare the D-type model with results of seismic modelling along the International Profile V described by Uchman (1975), and to look for analogies. In the crustal model for the profile V, trending N–S and crossing the PKB near the CEL04 and CEL05 profiles, there is a rectangular Moho depression of 10 km depth and 40 km length, with southern edge located at the PKB. Such a feature is a few times larger than the pseudo-diffractor modelled here, and shifted some 20 km to the North. However, taking into account different methodologies of modelling, both models may reflect the existence of the same type of structure at the crust-mantle boundary, interpreted in a different way.

Another argument for the superiority of the pseudo-diffractor model in case of D-type data are CEL04 recordings of few shots located in the opposite direction (to south-east from IWC), exhibiting also a high-velocity mantle phase. A north-dipping discontinuity would not reflect waves coming from the south, unlike a pseudo-diffractor, which should generate observable arrivals independently of the incident wave direction.

6 DISCUSSION AND CONCLUSIONS

The modelling showed that the uppermost mantle structure beneath the Western Carpathians can be described by two concurrent models, however there are hints that the R-type model seems to be more suitable for the western part, whereas in the east the D-type model is preferred.

The R-type model suggests the existence of the northward dipping, 1- to 5-km-thick discontinuity in the uppermost mantle below Carpathians. The velocity contrast at the reflector is hard to estimate with the method used, as a positive contrast of 0.5 and a 1.0 km s^{-1} negative contrast both produce synthetic data with a satisfactory amplitude relative to the P_n phase. The negative contrast ($V_p \sim$ 7.0 km s^{-1}) would imply either an existence of a shear zone, where the mantle rocks velocity is lowered due to mylonitization, a change of structure or hydratation (Fountain *et al.* 1984; Warner & McGeary 1987), or the presence of the crustal material (delaminated lower crust or subducted oceanic crust; Balling (2000)).

A positive contrast (V_p of *ca.* 8.5 km s^{-1}), would suggest an eclogitization of crustal rocks at mantle depths. The results of Hansen & Balling (2004) indicate that eclogitization (full or partial) of the crustal material submerged in the upper mantle can create an impedance contrast which is sufficient to generate strong reflected arrivals.

The lower crustal rocks could be introduced to the upper mantle either by northward subduction of the oceanic lithosphere, or by delamination of the ALCAPA continental lithosphere at the lower crustal level due to a collision, which terminated the Carpathian subduction (Fig. 6). Available geological evidence consistently supports the scenario of an opposite, southward Tertiary subduction of the European lithosphere beneath the ALCAPA, as the most prominent and widespread orogenic event, with a resulting suture at the

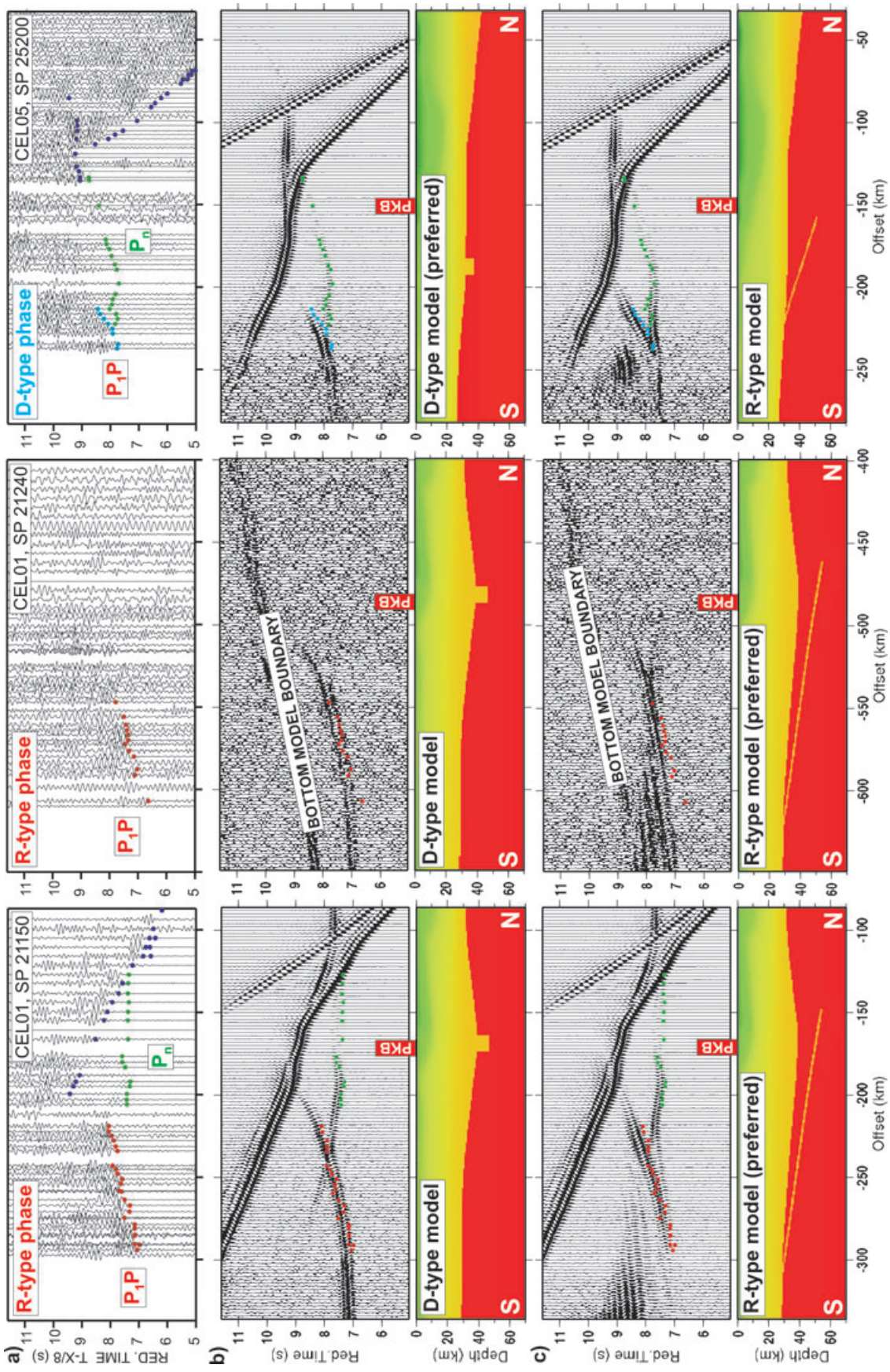

Figure 3. Examples of amplitude modelling. (a) Observed data, (b) D-type model and corresponding synthetic data and (c) R-type model and synthetic data. All sections are trace-normalized. Reduction velocity is 8 km s^{-1}.

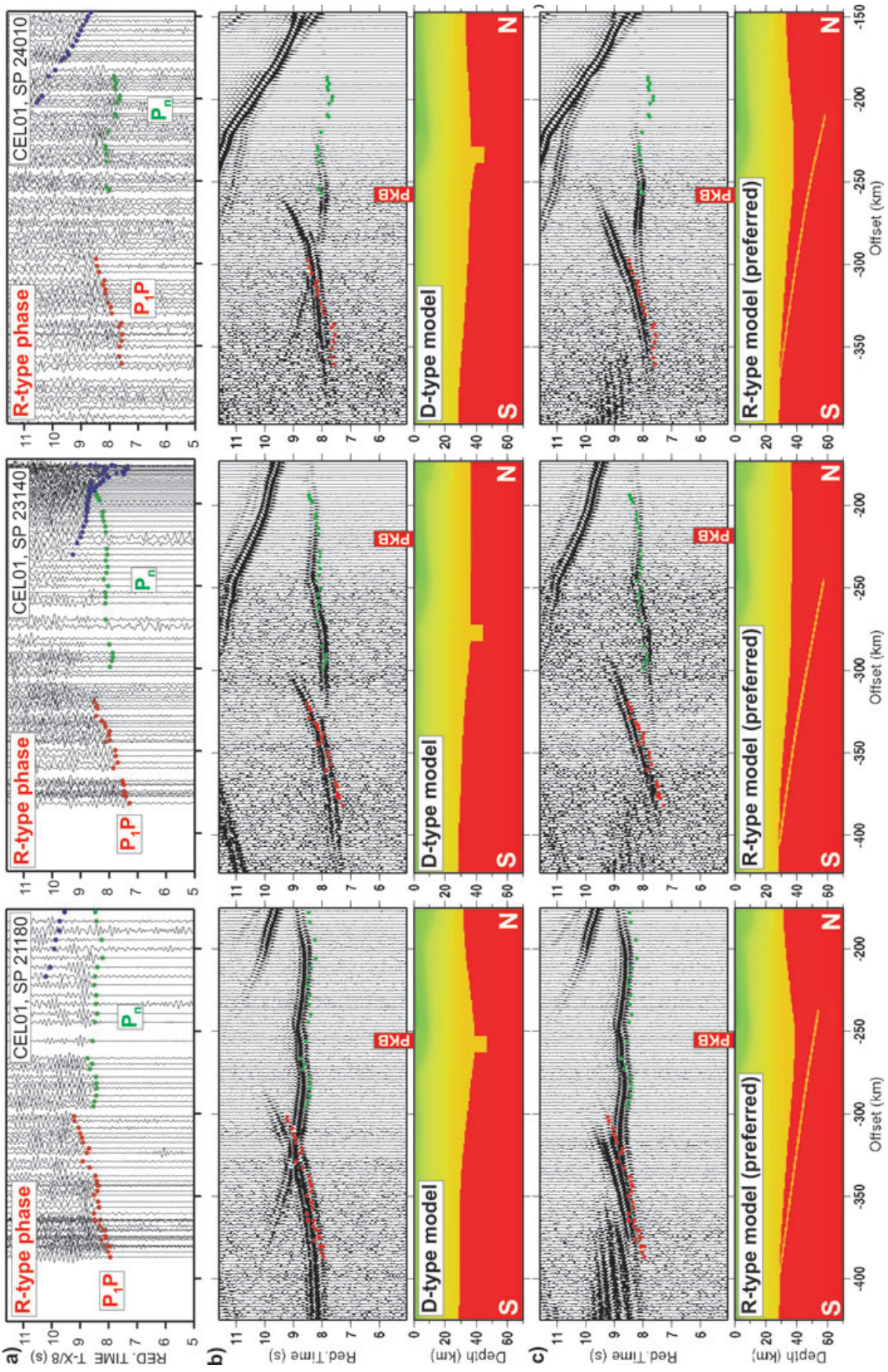

Figure 4. Examples of amplitude modelling of the R-type P_1P phase. (a) Observed data, (b) D-type model and corresponding synthetic data and (c) R-type model and synthetic data. All sections are trace-normalized. Reduction velocity is 8 km s^{-1}.

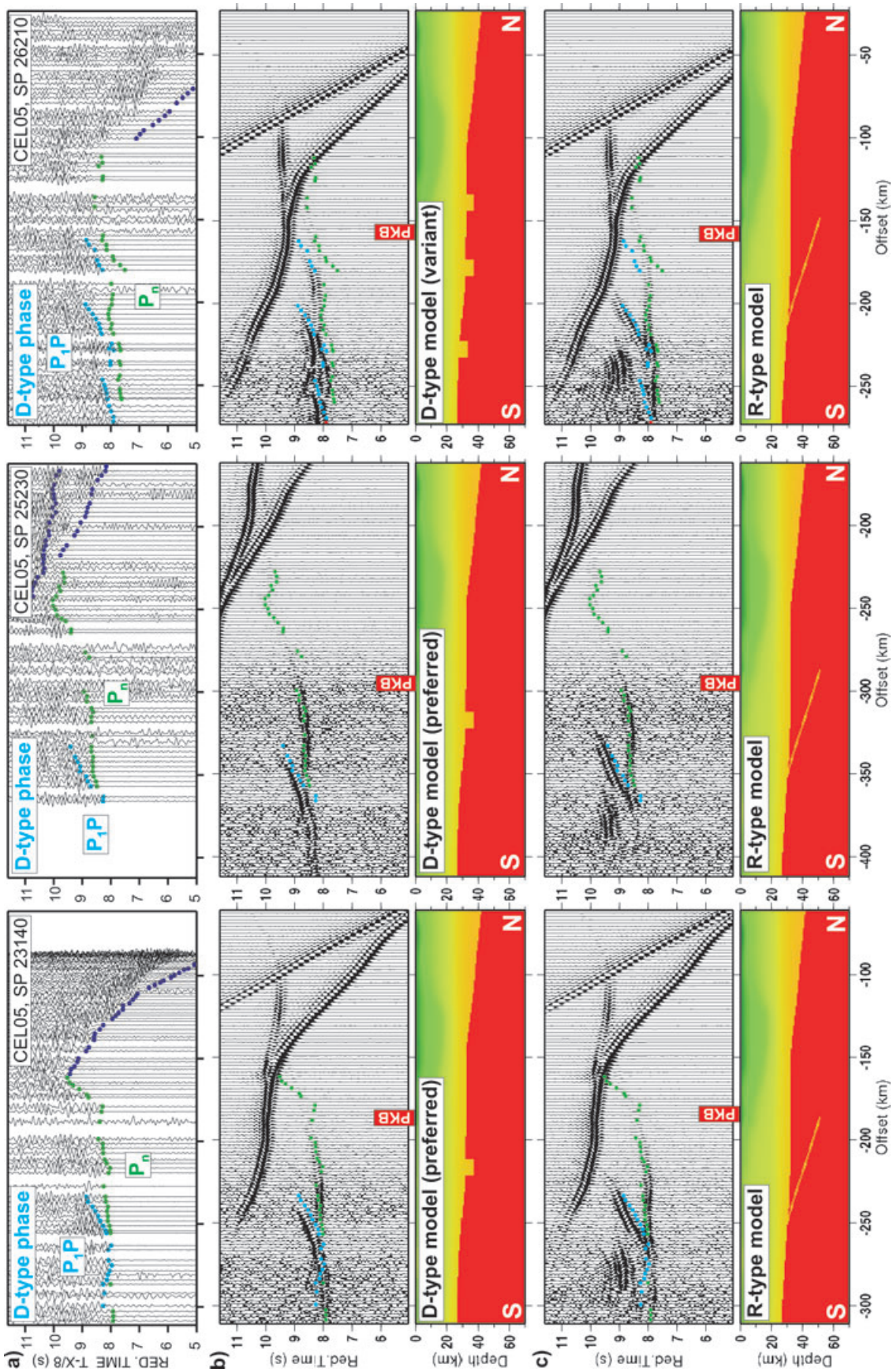

Figure 5. Examples of amplitude modelling of the D-type P_1P phase. (a) Observed data, (b) D-type model and corresponding synthetic data and (c) R-type model and synthetic data. All sections are trace-normalized. Reduction velocity is 8 km s^{-1}.

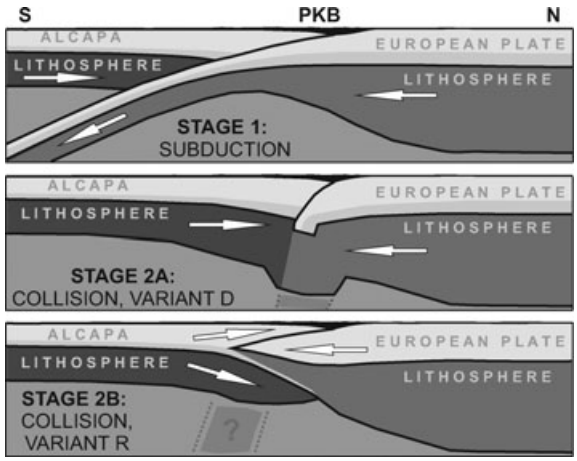

Figure 6. A cartoon showing possible tectonic interpretations of the 'bright spot' beneath the Western Carpathians.

PKB. Recently, Lippitsch *et al.* (2003), based on the tomographic evidence, suggested northward polarity of the Mid-Cretaceous to Early Tertiary Eastern Alpine subduction, close to the study area. However, the Western Carpathian subduction, occurring much later and resulting from NE lateral extrusion of ALCAPA triggered by the Eastern Alpine collision, did not have to occur in an analogous way.

When discussing the subduction polarity in the context of this work, it should be stressed that the northward subduction, which can be postulated based on the models presented here, would refer to another subduction episode than the Tertiary one, and at a different location. This is because the upward extension of the modeled mantle reflector reaches the surface not at the PKB, but 150–200 km south of it—near the HDL, roughly coinciding with the Meliata suture. Thus, such an interpretation of the mantle reflector does not provide grounds for negating the southward subduction of the European lithosphere at the PKB, and does not imply an opposite subduction polarity at this suture, unlike suggested by Lippitsch *et al*. (2003) for the Eastern Alps. Instead, as some authors (e.g. Golonka, 2004) consider the Meliata suture as the closure resulting from the Late Jurassic northward subduction of the Meliata-Halstatt oceanic lithosphere beneath Inner Carpathians, the N-dipping mantle reflector could be regarded as a trace of the corresponding subducted slab. However, such an interpretation leads to some contradictions (that I shall now consider) that make it questionable.

First, why is the image of the older (Jurassic) and spatially more limited subduction preserved and visible in seismic data, while there is no observable seismic evidence in the mantle for the more recent (Tertiary) and presumably more widespread European slab? Second, the southward subduction at the PKB, occurring later and affecting the same mantle region as the oppositely dipping Meliata slab, would involve movement across the line of the modelled reflector (assumed Meliata slab), thus destroying at least part of it, even in case of a steep-angle subduction at the PKB. Moreover, the subduction-related back-arc extension in the Inner Carpathians, together with associated widespread magmatic processes, should also considerably influence any older structures in the upper mantle, obliterating the Meliata slab.

Other preferred scenario of emplacement of the crustal rocks in the mantle involves ALCAPA lithosphere delamination at the lower crustal level. The extensive crustal shortening at the post-subduction collisional stage could lead to northward underthrusting of the delaminated ALCAPA lower crust and uppermost mantle beneath the wedge of rigid and strong European lithosphere and to the formation of a 'crocodile' structure (Fig. 6). Such collisional structures were proposed, for example by Meissner *et al.* (2002) and Snyder (2002). This process could create a North-dipping discontinuity with either a negative impedance contrast—due to the formation of a shear zone where alteration of rock structure decreases V_p velocity (Abramovitz *et al.* 1998; Krawczyk *et al.* 2002) and/or due to the presence of the lower crustal material in the mantle—or with a positive contrast, if the crustal material underwent eclogitization.

The D-type model—a low-velocity anomaly of the ∼10 km size at the base of the crust—may be interpreted as a fragment of the lower crustal material submerged in the mantle, representing a remnant of a subducted plate after the slab break-off (Fig. 6). The anomaly is located at a close (0–30 km) distance from the PKB, thought to represent the surface contact of plates. This suggests a steep-angle subduction of the oceanic European lithosphere, at least in the final stage. A subsequent collision led to the oceanic slab break-off, bending of the slab remnant and the formation of a subvertical plate contact, marked at the surface by the PKB and at the Moho level by the oceanic crust remnant. Such a scenario is consistent with the interpretation of Lexa & Konečný (1998) and Nemcok *et al.* (1998), who suggest subduction verticalization and slab tearing during the final subduction stage based on time and space relations of Neogene volcanites in the IWC.

Moreover, these studies present evidence for an eastward migration of the active subduction area (and progressive change to collision) along the Carpathian arc due to the oblique plate movement direction. Such a scenario strongly supports the proposed subdivision of the Western Carpathians into the R-type model in the West and D-type model in the East. In the western part, early onset of collision resulted in a more advanced collision stage in present, with extensive crustal shortening leading to ALCAPA lithosphere delamination and formation of a 'crocodile' structure, which fits the R-type model (Fig. 4). In the East, a later onset of collision involved less advanced deformations only, with moderate crustal shortening manifested solely by a verticalization of the slab remnant, represented by the D-type model. The variant of the D-type model with three pseudo-diffractors (Fig. 5, SP 26210) may suggest that in some places, the collision led to more complicated deformations of colliding crustal blocks, resulting in the creation of other low-velocity anomalies at the Moho level, both South and North of the PKB.

The modelling outcome leads also to important considerations concerning the non-uniqueness in seismic interpretation of a non-ideal dataset. Non-uniqueness is an inherent property of a solution of the seismic inverse problem, but is usually manifested (or understood) as quantitative uncertainty of determination of the velocity or depth to some structure, which does not influence the overall geological meaning of the model. The case presented here is of particular interest as it shows that in some cases, non-uniqueness can also lead to two qualitatively different solutions for the same dataset, suggesting the existence of structures of a dissimilar origin, and, as a consequence, to disparate tectonic implications.

The synthetic full waveform modelling showed that two contrasting kinds of structures generate seismic phases with similar properties, hard (or impossible) to distinguish from each other in real data, considering limited data density and the presence of noise.

The first class of structures is represented by a velocity discontinuity of a large (∼100 km) horizontal extent and a small (few km) thickness, suggesting a geologically meaningful contact between large-scale units in the lithosphere, and pointing to the

specific petrological and geodynamical processes of its creation. On the other hand, the second class involves a localized, small scale (∼10 km size) structure, which, as shown here, may be tectonically meaningful if correlated with other structures, but generally, due to its small size compared to the length scale of tectonic structures modelled by wide angle data (few hundreds of km), is usually meaningless in terms of geological interpretation, and in many cases can be even treated as a mere manifestation of the random heterogeneity of the lithosphere, carrying no useful information about the large-scale tectonic structure. An incorrect interpretation of such an equivoque data set may lead either to neglecting a major feature, or, even worse, to postulating an imaginary one. Therefore, care must be taken to supplement the seismic data with other information, which may help to discriminate between possible solutions.

ACKNOWLEDGMENTS

The GMT (Wessel & Smith 1995) and CWP/SU (Cohen & Stockwell 1997) packages were used for the preparation of the figures. The author thanks two anonymous reviewers for their valuable suggestions.

REFERENCES

Abramovitz, T., Thybo, H. & MONA LISA Working Group, 1998. Seismic structure across the Caledonian Deformation Front along MONA LISA profile 1 in the southeastern North Sea, *Tectonophysics,* **288,** 153–176.

Babuška, V. & Plomerová, J., 2006. European mantle lithosphere assembled from rigid microplates with inherited seismic anisotropy, *Phys. Earth planet. Inter.,* **158**(2–4), 264–280.

Balling N., 2000. Deep seismic reflection evidence for ancient subduction and collision zones within the continental lithosphere of northwestern Europe, *Tectonophysics,* **329,** 269–300.

Cohen, J.K. & Stockwell, J.W. Jr., 1997. CWP/SU: Seismic Unix Release 30: a free package for seismic research and processing, Center for Wave Phenomena, Colorado School of Mines.

Červený, V. & Pšenčík, I., 1983. SEIS83 – numerical modelling of seismic wave fields in 2-D laterally varying layered structure by the ray method, in *Documentation of Earthquake Algorithm,* pp. 36–40, ed. Engdahl, E.R. World Data Center A for Solid Earth Geophys, Boulder, Rep. SE-35,

Fountain, D.M., Hurich, C.A. & Smithson, S.B., 1984. Seismic reflectivity of mylonite zones in the crust, *Geology,* **12,** 195–198.

Golonka, J., 2004. Plate tectonic evolution of the southern margin of Eurasia in the Mesozoic and Cenozoic, *Tectonophysics,* **381,** 235–273.

Grad, M. *et al*., 2006. Lithospheric structure beneath trans-Carpathian transect from Precambrian platform to Pannonian basin: CELEBRATION 2000 seismic profile CEL05. *J. geophys. Res.,* **111**(B3301), doi:10.1029/2005JB003647.

Guterch, A., Grad, M. & Keller, G.R., 2001. Seismologists celebrate the new millennium with an experiment in Central Europe, *EOS Trans. Am. geophys. Un.,* **82**(45), 529,534–535.

Hansen, T.M. & Balling, N., 2004. Upper-mantle reflectors: modelling of seismic wavefield characteristics and tectonic implications, *Geophys. J. Int.,* **157,** 664–682.

Hansen, T.M. & Jacobsen, B.H., 2002. Efficient finite difference waveform modeling of selected phases using a moving zone, *Comput. Geosci.,* **28**(7), 819–826.

Janik, T., Grad, M., Guterch, A. & CELEBRATION 2000 Working Group, 2009. Seismic structure of the lithosphere between the East European Craton and the Carpathians from the net of CELEBRATION 2000 profiles in SE Poland, *Geol. Quart.,* **53**(1), 141–158.

Kováč, M., Bielik, M., Pereszlényi, M., Šefara, I., Túnyi, I. & Vass, D., 1997. The Western Carpathian intramontane basins, in *Geological Evolution of the Western Carpathians. Mineralia Slov. Monograph,* 1–24, eds. Grecula, P., Hovorka, D. & Putiš M., GSSR, Bratislava.

Krawczyk, C.M., Eilts, F., Lassen, A. & Thybo, H., 2002. Seismic evidence of Caledonian deformed crust and uppermost mantle structures in the northern part of the Trans-European Suture Zone (TESZ), SW Baltic Sea, *Tectonophysics,* **360,** 215–244.

Lexa, J. & Konečný, V., 1998. Geodynamic aspects of the neogene to quaternary volcanism, in *Geodynamic development of the Western Carpathians,* pp. 143–154, ed. Rakús M., GSSR, Bratislava.

Lippitsch, R., Kissling, E. & Ansorge, J., 2003. Upper mantle structure beneath the Alpine orogen from high-resolution teleseismic tomography, *J. geophys. Res.,* **108**(B8), 2376, doi:10.1029/2002JB002016.

Mahel', M., 1981. Island character of Klippen Belt; Vahicum—continuation of Southern Penninicum in West Carpathians, *Geol. Zb.-Geol. Carpath.,* **32,** 293–305.

Nemcok M., Pospíšil, L., Lexa, J. & Donelick R.A., 1998. Tertiary subduction and slab break-off model of the Carpathian–Pannonian region, *Tectonophysics,* **295,** 307–340.

Meissner, R., Thybo, H. & Abramovitz, T.J., 2002. Interwedging and inversion structures around the Trans European Suture Zone in the Baltic Sea, a manifestation of compressive tectonic phases, *Tectonophysics,* **360,** 265–280.

Plašienka, D., Grecula, P., Putiš, M., Kovác, M. & Hovorka, D., 1997a. Evolution and structure of the Western Carpathians: an overview, in *Geological evolution of the Western Carpathians,* Mineralia Slovaca – Monograph, 1–24, eds. Grecula, P., Hovorka, D. & Putiš M., GSSR, Bratislava.

Plašienka, D., Putiš, M., Kováč, M., Šefara, J. & Hrušecký, A., 1997b. Zones of Alpidic subduction and crustal underthrusting in the Western Carpathians, in *Geological Evolution of the Western Carpathians,* Mineralia Slovaca – Monograph, 1–24, eds. Grecula, P., Hovorka, D. & Putiš M., GSSR, Bratislava.

Snyder, D.B., 2002. Lithospheric growth at margins of cratons, *Tectonophysics,* **355,** 7–22.

Środa, P. *et al*., 2006. Crustal and upper mantle structure of the Western Carpathians from CELEBRATION 2000 profiles CEL01 and CEL04: seismic models and geological implications, *Geophys. J. Int.,* **167,** 737–760.

Tomek Č. & Hall, J., 1993. Subducted continental margin imaged in the Carpathian of Czechoslovakia, *Geology,* **21,** 535–538.

Uchman, J., 1975. Tectonic characteristics of the region of International Profile V of deep seismic sounding in the Outer Carpathians and Foreland, *Publs. Inst. Geoph. Pol. Ac. Sci.,* **82,** 111–118.

Warner, M. & McGeary, S., 1987. Seismic reflection coefficients from mantle fault zones, *Geophys. J. R. astr. Soc.,* **89,** 223–230.

Wessel, P. & Smith, W.H.F., 1995. New version of Generic Mapping Tools released, *EOS, Trans. Am. geophys. Un.,* **76,** 329.

Zeyen, H., Dererová, J. & Bielik, M., 2002. Determination of the continental lithospheric structure in the Western Carpathians: integrated modelling of surface heatflow, gravity anomalies and topography, *Phys. Earth planet. Inter.,* **134,** 89–104.